PCCP

Accepted Manuscript

ROYAL SOCIETY OF CHEMISTRY

www.rsc.org/pccp

Cite this: DOI: 10.1039/c0xx00000x

www.rsc.org/xxxxxx

ARTICLE TYPE

Supramolecular amphipathicity for probing antimicrobial propensity of host defence peptides

Jascindra Ravi,[a,‡] Angelo Bella,[a,‡] Ana J. V. Correia,[a,b] Baptiste Lamarre [a] and Maxim G. Ryadnov*[a]

Received (in XXX, XXX) Xth XXXXXXXXX 20XX, Accepted Xth XXXXXXXXX 20XX

DOI: 10.1039/b000000x

Host defence peptides (HDPs) are effector components of innate immunity that provide defence against pathogens. These are small-to-medium sized proteins which fold into amphipathic conformations toxic to microbial membranes. Here we explore the concept of supramolecular amphipathicity for probing antimicrobial propensity of HDPs using elementary HDP-like amphiphiles. Such amphiphiles are individually inactive, but when ordered into microscopic micellar assemblies, respond to membrane binding according to the orthogonal type of their primary structure. The study demonstrates that inducible supramolecular amphipathicity can discriminate against bacterial growth and colonisation thereby offering a physico-chemical rationale for tuneable targeting of biological membranes.

Introduction

Physico-chemical mechanisms that can discriminate against microorganisms are of fundamental importance to molecular medicine and biomaterial design.[1] With the rise of bacterial cross-resistance to conventional antibiotics, novel approaches are sought to provide efficient solutions for antimicrobial prevention and intervention.[2] Of particular interest are those strategies that exploit differences in microbial and mammalian membranes.[3] Examples include protein extracellular matrices[4] and metal nanopatterned surfaces[5] that exhibit differential responses to cell adhesion and colonisation or biofilm-resistant polymer coatings[6] and hydrogels.[7] Nature often is the source of inspiration with offers ranging from self-decontaminating insect wings[8] to antimicrobial protein nanonets.[9] Notably, universal physico-chemical principles of antimicrobial responses are programmed in the effector molecules of the innate immune system found in all multicellular organisms.[10]

Usually referred to as host defence peptides (HDPs),[10] such molecules recognise and disrupt microbial membranes – the ability which directly correlates with their oligomerisation characteristics.[11] Specifically, the peptides fold into amphipathic conformations in response to membrane binding, which allows them to assemble into pores[11] or carpet-like structures.[12] In some instances, HDPs can aggregate in solution which may render them cytotoxic. However, the persistent order of individually inactive HDP-like amphiphiles into supramolecular structures, reported for native[9] and synthetic[4] systems, proves to support antimicrobial activity. This phenomenon prompts the conjecture of applying supramolecular order to probing the antimicrobial propensity of elementary HDP moieties that alone cannot support appreciable activity. Here we probe such a conjecture by design.

Results and discussion

Supramolecular peptide design

HDPs exhibit generic structural parameters which allows their modulation in synthetic sequences.[3] Typically, the peptides comprise about equal numbers of cationic and hydrophobic amino-acid residues, which upon binding to anionic microbial surfaces partition into two opposite clusters. This leads to the formation of secondary amphiphiles – secondary structures, β-sheets or α-helices, with distinctive cationic and hydrophobic faces made of cationic lysines or arginines and hydrophobic residues such as leucines, valines or isoleucines.[11, 13] Thus, the smallest or elementary HDPs (eHDPs) would be a two-residue sequence comprising single hydrophobic and cationic residues. Such a sequence would not fold into a secondary amphiphile and has to self-oligomerise to form sufficiently extensive faces of amino-acid side chains to contact with microbial surfaces.[4, 9] In this regard, an eHDP moiety derivatised with an aliphatic domain can provide a straightforward model.[14] The domain enables the peptide to spontaneously assemble into elongated micellar structures, the assembly of which is driven by the burial of aliphatic chains in the core, with peptide moieties displayed on the periphery (Figure 1).

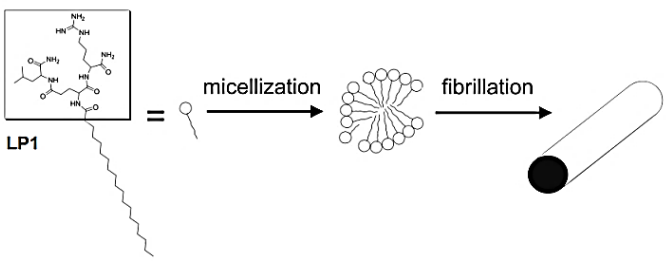

Figure 1. Schematic representation of a lipopeptide (LP), comprising an eHDP (squared, LP1) with an aliphatic (C18) domain, and the assembly of the peptide into fibrillar micelles.

Assembled micelles are microns-long high aspect-ratio fibrils in which the cationic and hydrophobic side chains of eHDPs form extended coronae surfaces.[4, 14] The eHDPs are aligned and conformationally locked into persistent elongated seams of electrostatic and hydrophobic faces exposed to bacterial

attachment.[9] Antimicrobial activity is defined by the formation of such seams and by the propensity of eHDPs to form these.

To probe this rationale, we generated two versions of lipo-eHDPs. In one, a glutamate residue was used as a hub to form an isopeptide bond at its side chain with a hydrophobic leucine and a standard peptide bond with a cationic arginine thus giving rise to a branched Q(L)R. Arginine was chosen over lysine to arrange stronger electrostatic interactions, which may prove crucial for membrane binding. Leucine has a lower hydropathy score than isoleucine and valine, and was preferred to minimise solubility issues.

Another eHDP was a linear QLR sequence. Each of these eHDP units was linked to an aliphatic (C18) chain at the N-terminus (Figure 1 and Table 1).

The resulting branched and linear lipopeptides, LP1 and LP2 respectively, present two orthogonal modes of side-chain exposure on micellar surfaces (Figure 1). This allows probing antimicrobial activity as a function of tertiary contacts between microbial membranes and the elongated seams which may differ for branched and linear eHDPs only in folding patterns.

Table 1. Peptide constructs[a] used in the study

Name	Structure
LP1	C_{18}-Q(L)R
LP2	C_{18}-QLR
LP3	C_{18}-CGCQ(L)R
LP4	C_{18}-CGCQLR
LH	C_{12}-$(\beta A)_2$-KIAKLKAKIQKLKQKIAKLK

[a] all are C-terminal amides

Supramolecular amphipathicity and membrane binding

Indeed, transmission electron microscopy (TEM) revealed morphologically similar fibrillar structures for LP1 and LP2 (Figure 2). However, the structural backgrounds of the two modes were distinctively different.

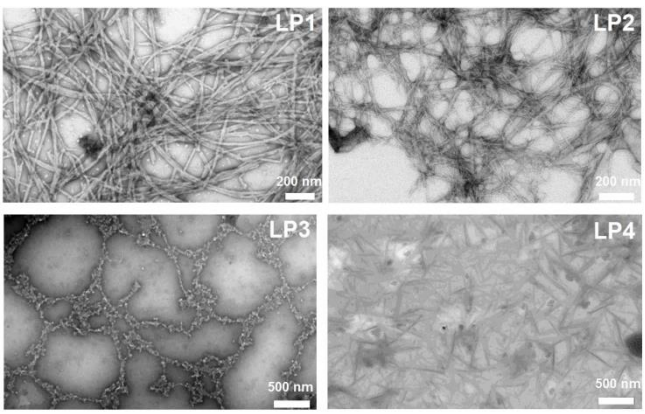

Figure 2. Electron micrographs of LP1-LP4 (100 μM) in 10 mM MOPS, pH 7.4, overnight incubation at room temperature.

Specifically, circular dichroism (CD) spectra for LP1 were dominated by random coil conformations with elements of β-turn structure.[15] In contrast, LP2 appeared characteristically helical with signal dampening towards lower wavelengths which is commonly observed for self-assembled systems (Figure 3A).[16]

The result is intriguing in that LP2 falls short of a single helical turn (3.6 residues) and cannot fold into a helix alone. Therefore, it can be attributed to the ordering of the peptide into persistent, albeit non-covalent, QLR chains in fibrillar micelles that may induce helix-like folding to the extent observed (<5%).[17]

It should be noted here that this scenario would only be possible if eHDP units in fibrils are aligned. Linear dichroism (LD) spectroscopy, which applies shear flow to probe the alignment of chromophores (peptide bonds), showed relatively strong absorbance bands for LP2 fibrils at 200-240 nm, which is

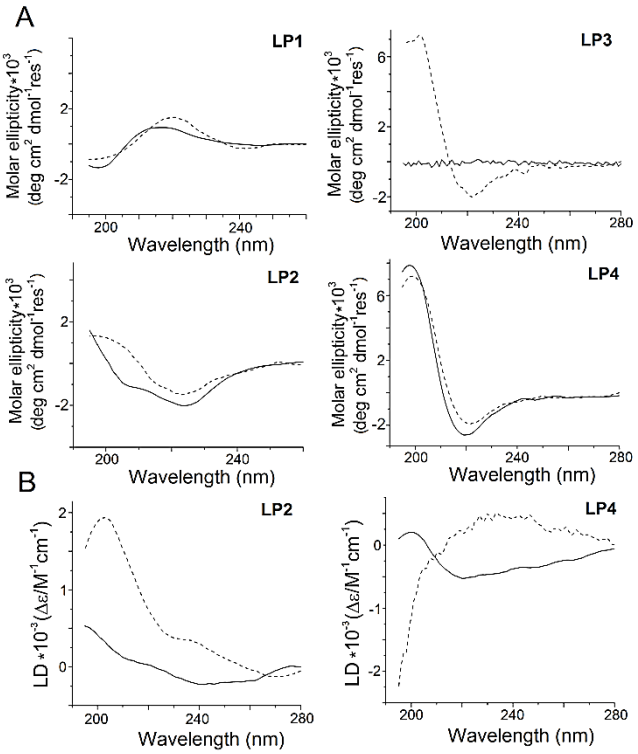

indicative of the aligned peptide backbone (Figure 3B).[18]

Figure 3. Circular dichroism (A) and linear dichroism (B) spectra of lipopeptides (100 μM) in 10 mM MOPS (solid line) and in the presence of anionic phospholipid vesicles (dashed line) at 1:30 peptide-lipid ratio.

Further insight came from LD spectra in the presence of anionic phospholipid vesicles used as microbial membrane mimetics.[11] A combination of two minima, at 195 nm and 220-230 nm, and a maximum, at 202-208 nm, recorded for LP2 was characteristic of α-helices oriented more parallel to the membrane surface (Figure 3B).[18] Yet, increased signal flattening at 208 nm in CD spectra may imply a membrane-induced conformational transition towards β-sheet structures.[19] This appeared consistent with that the LD spectra were dominated by the maximum, which can be observed for β-sheets laying on the membrane surface and for aligned amyloid fibrils.[18,20] Taken together the results suggest that LP2 should be conformationally plastic and responsive to immediate environments, but subjected to the alignment of eHDPs. In comparison, the conformational background of LP1 fibrils remained unchanged (Figure 3A) pointing to a greater conformational flexibility of LP1 monomers (isopeptide bonds of

branched Q(L)R) enabling a larger space of allowed conformations for LP1. Notably, however, in both cases similar microns-long and abundant fibrils were observed (Figure 2). Further constraining of eHDPs may result in reduced plasticity while exposing intrinsic conformations, which can lead to constrained micellisation with individually smaller or more dense and networked structures.[21]

Supramolecular order under constrained conformational plasticity

With this in mind, LP1 and LP2 were extended at their N-termini with a cysteine-containing CGC motif to enable proximity-driven crosslinking between eHDPs (Table 1).[21] As gauged by TEM, the resulting LP3 and LP4, modified LP1 and LP2 respectively, assembled into two distinct morphologies featured with amorphous network-like (LP3) and fibrillar carpet-like (LP4) formations of apparently smaller structures (Figure 2). The comparative quantification of free thiols by the Ellman's test gave up to 70% reductions in the concentration of free thiols when compared before and after the assembly, which agrees well with that in peptide self-assembled structures ~70% of monomers are incorporated into the assembly.[22] This finding infers that cysteine residues of the eHDPs were oxidised.

As expected, no signals were detected by LD spectroscopy for LP3 which lacked elongated structures that could align, whereas LD spectra for LP4 were similar to those reported for amyloid-like fibrils suggesting that β-strands are oriented perpendicular to the main fibril axis (Figure 3B).[20] Complementarily, CD spectra for LP4 were typical of β-pleated structures and remained such in the presence of synthetic membranes (Figure 3A), while LD spectra were consistent with a perpendicular orientation of β-sheets to membrane surfaces (Figure 3B).[18] Intriguing was the response of LP3 to membrane binding. While no structure could be ascertained for LP3 in solution, appreciable β-sheet CD signals were obtained in the presence of the membranes (Figure 3A).

Collectively, these results support the conjecture of a greater plasticity for the branched orthogonal eHDPs, LP1 and LP3, and suggest membrane-induced structural responses for both orthogonal modes.

An outstanding question related to these conclusions is whether the observed behaviours are exclusive for lipopeptides with intrinsic propensity for β-sheet structure or can be applied to full-length HDPs based on a different folding motif. To test this, two sets of experiments were performed. In one, C18 chains in LP1-LP4 were replaced by shorter C12 domains, which were to reduce the contribution of lipid domains to self-assembly, thus further probing the propensity of eHDPs to fold. For another set, a previously reported α-helical 20-mer HDP[11,23] was used as a conjugate with a C12 lipid domain via a two-βAla spacer (Table 1 and Figure 4A).

None of the C12-based peptides folded or assembled. This could be expected as, unless sufficiently restrained, the conformational plasticity of eHDPs would compromise assembly and in turn peptide alignment and folding.

In case of the α-helical lipopeptide, dubbed lipohelix (LH), the plasticity is defined by a transition from random coil to helical conformations which is induced by interactions with phospholipid membranes.[23] Like LP1, LH does not have to fold to micellise, but due to its strongly amphipathic structure it is to fold in response to membrane binding in a fashion analogous to that of LP2 or LP3. Irrespective of this, the 20-mer HDP is likely to maintain its alignment in the assembly without disintegrating. Questions however remain as to the orientation of HDP in relation to membrane surfaces.

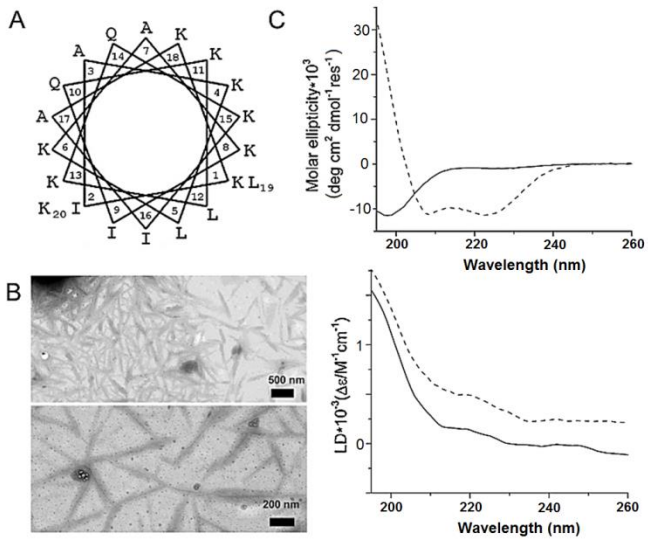

Figure 4. Lipohelix (LH). (A) HDP sequence configured into a helical wheel. (B) Electron micrographs of LH (100 μM) in 10 mM MOPS, pH 7.4, incubation overnight. (C) Circular dichroism (upper) and linear dichroism (lower) spectra of LH (100 μM) in 10 mM MOPS (solid line) and in the presence of anionic phospholipid vesicles (dashed line) at 1:30 peptide-lipid ratio.

TEM confirmed the assembly of LH into fibrillar micelles with morphological and dimensional characteristics of the other fibrils (Figure 4B). This indeed was not accompanied by appreciable folding as judged by CD spectra, and gave strong LD signals indicating that the peptide backbone in LH micelles was aligned.[18] Interestingly, the alignment did not change in the presence of phospholipid membranes, while strong helical signals (~30% helix)[17] when compared to those for LP2 were recorded by CD spectroscopy confirming membrane-mediated folding. LD spectral features for LH-membrane mixtures were interpretable as α-helices oriented more perpendicular to the membrane surfaces.[18, 23] This is consistent with helices oriented perpendicular to the main fibril axis, possibly due to contributions from irregular para-helical regions,[24] but may largely reflect that the HDPs in fibrils are aligned (Figure 4C).

Combined the data supports two main conclusions. Firstly, supramolecular order, namely fibril-like micellisation, can be used to expose specific folding propensities and conformational responses to membrane binding of elementary HDP units. Secondly, these parameters, i.e. folding propensity and responsiveness, are consistent with the behaviour of full-length HDPs irrespective of folding preferences and independent of the contribution of lipid domains, the role of which is confined to micellisation.

A subsequent reasoning on how these may relate to antimicrobial activity was probed directly using biological tests.

Supramolecular order and biological activity

The outlined experimental design applied supramolecular assembly to amplify the intrinsic antimicrobial activity of individually inactive eHDPs, while for LH any substantial change in activity compared to the HDP was not expected.

The side chains of assembled eHDPs form continuous amphipathic seams in LP fibrils which can be viewed as antimicrobial "carpets". Such carpets span microscopic dimensions and therefore should prove resistant against bacterial adhesion and colonisation. It is also envisaged that structural differences observed in LP1-LP4 may correlate with different biological responses.

In this light, all LPs were used as adhesion substrates for the adhesion of *P. aeruginosa*, *E. coli* and *S. aureus*. Bacteria were incubated over 16 hours, the first most critical hours for bacterial colonisation,[25] and were then visualised by fluorescence microscopy (Figure 5A).

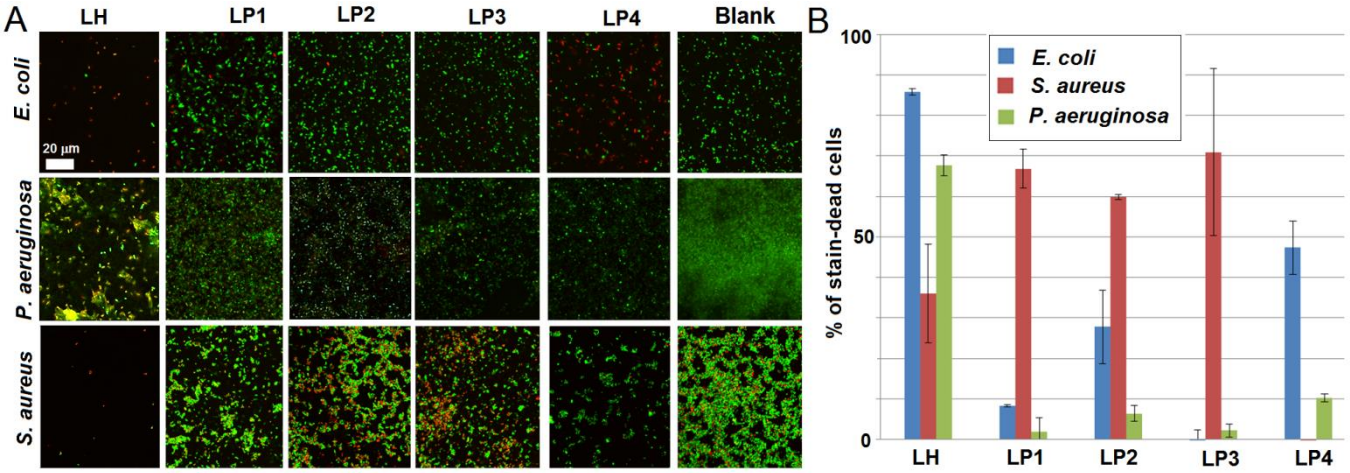

Figure 5. Biofilm resistance of LP1-4 and LH. (A) Representative fluorescence micrographs of *P. aeruginosa*, *E. coli* and *S. aureus* after 16-hour incubations on different substrates. Live/dead staining was used to label live (green) and dead (red) bacteria. (B) total dead cell count given as a percentage of total cell count after subtracting the background adhesion (bare substrate). Note: no visible fluorescence (LH) denotes antimicrobial effects at both levels – individual monomers (killing before bacterial adhesion) and as fibrillar assemblies (killing upon bacterial adhesion). Yellow fluorescence derives from overlapping live (green) and dead (red) bacteria.

LP1-LP3 showed no apparent activity against *P. aeruginosa*, whereas LP2 was moderately active against *E. coli*. All three substrates induced strong antimicrobial effects against *S. aureus* (Figure 5B). The tendency was reversed to that observed for LH, which gave comparatively weaker responses against *S. aureus* than against the other two bacteria. Strikingly, LP4 was nearly selective against *E. coli* with marginally higher activity against *P. aeruginosa* when compared to LP1-LP3. These findings were in good agreement with the results from microdilution assays, used to determine minimum inhibitory concentrations (MICs) of individual peptides. Consistent with the design concept, none of the LPs was found active (>100 μM), in both C12 and C18 forms, while MICs for the LH were typical of those for full-length HDPs (Table 2).[3, 11-13]

Table 2. Biological activity of the constructs used in the study[a]

Name	Minimum inhibitory concentrations (MIC), μM			(LC_{50})[b], μM
	P. aeruginosa (ATCC27853)	*S. aureus* (ATCC6538)	*E. coli* (K12)	Mammalian erythrocytes
LP1	>100	>100	>100	>>100
LP2	>100	>100	>100	>>100
LP3	>100	>100	>100	>>100
LP4	>100	>100	>100	>>100
LH	5.73±0.07[b]	23.69±0.22	12.24±1.65	>>100

[a]similar results were found for C12-based eHDPs; [b]50% cell death compared with untreated cells, <3% at 100 μM.

The antimicrobial effects observed for LPs were arranged by ordered micellisation indicating resistance against bacterial adhesion rather than a purely killing mechanism.[6, 8] The latter would require an inhibitory activity of an antibiotic engaging with a specific intracellular target (e.g. ribosome, translation factor) or direct membrane disruption. The LP sequences are not antibiotics, and are too short to fold autonomously and oligomerize into membrane-disrupting structures. Therefore, their activity requires pre-concentration or pre-organisation into supramolecular assemblies that, proven responsive to membrane binding, would act against bacterial membranes upon contact.

LH is antimicrobial at both levels tested. Its activity does not depend on the ability to assemble and is determined by monomers,[30] which can attack bacterial membranes via a diffusion mechanism characteristic of HDPs.[11] When pre-assembled into supramolecular structures the monomers arrange into extensive amphipathic surfaces able to repel bacterial adhesion.[4] As a consequence, LH exhibits comparable activities against different bacteria with close correlations between MIC and adhesion assays (Table 1 and Figure 5B).

The biological activity of LPs is delivered only at the supramolecular level, as pre-organised micelles, and hence must correlate with their folding responses to membrane binding (monomer alignment and orientation), the orthogonal type of their monomers (branched or linear) and their ability to assemble. Such a supramolecular rationale is demonstrated in clear tendencies of LP1-LP3 being more active against *S. aureus*, which may be attributed to their selectivity against Gram positive

membranes, and those of LP4 being active only against Gram negative bacteria. These differences derive from structural differences of the corresponding assemblies.

Indeed, LP4 appears to be the only system whose folding characteristics were constant. It formed β-structured fibrils which did not undergo conformational changes, with β-strands likely to run perpendicular to the fibril axis while retaining orientation in contact with membranes (Figure 3). These properties conformed to an amyloid-like structure.[26] Amyloid components are known to bind to lipopolysaccharides of Gram negative bacteria,[27] while amyloid fibrils can be formed by Gram-positive bacteria (*Streptomyces*) to promote the growth of aerial hyphae and cytotoxicity to the extracellular space.[28] Although such reports suggest a degree of specificity of amyloid assemblies towards Gram-negative membranes there exist no strict correlations for their preferential targeting.[29]

LP2 and LP3 assemblies are not constant and therefore are likely to be subject to equilibrium fluctuations suggesting the release of low oligomers that provide conformation-responsive cytotoxic effects. LP1 has no well-defined structure, but has nearly identical assembly characteristics compared to LP2 fibrils, which together with the comparable activities of these two systems implies similar equilibrium-dependent behaviours.

LP4 is different in that it is conformationally stable and may remain at a mechanical equilibrium lacking low oligomeric forms in any given time. Its action is that of a mechanical response to motile bacteria, *E. coli* and *P. aeruginosa*, but not to non-motile *S. aureus*, suggesting a physical mechanism akin to those for cicada-like nanopatterned surfaces.[5]

In summary, if eHDPs exhibit antimicrobial activities, however negligible (Table 2), these would amplify in their supramolecular assemblies where their antimicrobial propensity can become pronounced.

Conclusions

All in all, the results demonstrate that artificial supramolecular systems endowed with inducible amphipathicity can be designed to discriminate against bacterial growth. The findings support a mechanism of "supramolecular amphipathicity" which occurs via the formation of persistent cationic and hydrophobic faces. The extent of these faces and their reversibility accommodate antimicrobial effects for otherwise individually inactive HDPs units. These elementary HDPs are ordered into microscopic micellar assemblies as peripheral units, which respond to membrane binding according to the orthogonal type of their primary structure, which permits the use of supramolecular order for probing antimicrobial propensity of elementary HDP.

By exploiting the structural basis by which HDP prefer targeting bacteria over eukaryotic membranes the described concept permits further studies as to the precise mechanisms of action under equilibrium and non-equilibrium conditions, which are anticipated to lead to tuneable membrane-active systems capable of specifically targeting biological surfaces and interfaces.

Experimental

Peptide synthesis and mass-spectrometry

Peptide syntheses were performed on a Liberty system (CEM Corporation). The peptides were assembled on a rink amide MBHA resin (100 µM scale) using standard solid-phase Fmoc-based protocols with HBTU/DIPEA as coupling reagents. Fmoc-Glu(OH)-OAll was used as a C-terminal residue attached via its γ-carboxyl to assemble LP1 and LP3. Upon cleavage and deprotection (95% TFA, 2.5% TIS, 2.5% EDT) this Glu was converted into Gln. Synthesized peptides were purified by RP-HPLC following post-synthetic deprotection and work-up. The final constructs were identified by MALDI-ToF mass-spectrometry with α-cyano-4-hydroxycinnamic acid as the matrix:

MS $[M+H]^+$: LP1 – m/z 680.99 (calc), 682.63 (found); LP2 – m/z 680.99 (calc), 682.33 (found); LP3 – m/z 944.33 (calc), 945. 93 (found); LP4 – m/z 944.33 (calc), 944.68 (found); LH – m/z 2643.52 (calc), 2644.55 (found).

High performance liquid chromatography

Analytical and semi-preparative gradient RP-HPLC was performed on a JASCO HPLC system using Vydac C8 analytical (5 µm) and semi-preparative (5 µm) columns. Both analytical and semi-preparative runs used a 10-60% B gradient over 50 min at 1 mL/min and 4.7 mL/min respectively with detection at 230 and 220 nm. Buffer A – 5% and buffer B –95% aqueous CH_3CN, 0.1% TFA.

Synthetic membranes

1,2-dilauroylphosphatidylcholine (DLPC) and 1,2-dilauroyl-sn-glycero-3-phospho-(1-rac-glycerol) (DLPG), 75%/25% (w:w) (all from Avanti Polar Lipids) were used for the construction of anionic phospholipid vesicles. This combination provides fluid-phase discrete lipid bilayers (liposomes) at room and physiological temperatures that mimic microbial membranes and efficiently expose folding-mediated peptide-lipid interactions.[11,19] The lipids were dissolved in chloroform−methanol (2:1, v:v) and dried under a nitrogen stream before placing them under vacuum overnight. Resulting films were hydrated to 10 mg/mL total lipid concentration in 10 mM phosphate buffer, pH 7.4. The suspension was then extensively vortexed and sonicated (30 °C) before extrusion (15 times) through polycarbonate filters (0.05 µm) with a hand-held extruder (Avanti Polar Lipids). A clear solution containing small unilamellar vesicles (50 nm) was obtained and analyzed by photon correlation spectroscopy.

Photon correlation spectroscopy

Vesicles were re-suspended to final concentrations of 0.5-1 mg/mL and were analysed on a Zetasizer Nano (ZEN3600, Malvern Instruments, Worcestershire, UK). Hydrodynamic radii were obtained through the fitting of autocorrelation data to a single exponential function using the manufacture's Dispersion Technology Software (DTS version 5.10).

UV-visible spectroscopy

UV/vis measurements were carried out at room temperature in water on a Perkin Elmer Lambda 850 spectrometer to determine peptide concentrations. Absorptions at 214 were used. The extinction coefficients were calculated as described elsewhere.[31]

Circular and linear dichroism spectroscopy

Aqueous peptide solutions at 100 µM (300 µL) were prepared in filtered (0.22 µm) 10 mM MOPS, pH 7.4, at 20°C. Stock

solutions for LP1, LP2 and LH were in water (0.22 µm), LP3 and LP4 were in 1 mM TCEP. CD experiments were performed on a JASCO J-810 spectropolarimeter fitted with a Peltier temperature controller. All measurements were taken in ellipticities in mdeg and after baseline correction were converted to molar ellipticity (deg cm^2 dmol res^{-1}) by normalizing for the concentration of peptide bonds and cuvette path length. The percent α-helix was determined using an equation: $-100([\Theta]_{222} + 3000)/33\,000$.[17]

Solution-phase flow linear dichroism spectroscopy was performed on a Jasco-810 spectropolarimeter using a photo elastic modulator 1/2 wave plate. A micro-volume quartz Couette flow cell with ~0.5 mm annular gap and quartz capillaries were used (all from Kromatec Ltd, UK). Molecular alignment was achieved by applying the constant flow of the sample solution between two coaxial cylinders, a stationary quartz rod and a rotating cylindrical capillary. LD spectra were acquired with laminar flow obtained by maintaining the rotation speed at 3000 rpm and processed by subtracting non-rotating baseline spectra.

CD and LD spectra recorded in the presence of synthetic membranes are for lipid/peptide ratio of 30:1.

Transmission electron microscopy

Peptide solutions (200 µL, 100 µM) were incubated overnight in filtered (0.22 µm) 10 mM MOPS, pH 7.4, at 20°C. Following incubation an aliquot (25 µL) was applied for 5 min to a formvar/carbon coated copper/palladium grid subjected to plasma glow discharge. An excess solution was blotted away and the sample stained with 2% phosphotungstic acid was then visualised using Philips BioTwin transmission electron microscope at the accelerating voltage of 80 kV. The images were acquired with a fitted camera.

Determination of free thiols

A stock solution of 5,5'-Dithio-bis(2-nitrobenzoic acid) (Ellman's reagent) was prepared to a final concentration of 2mM in LC-MS grade water with 50 mM sodium acetate. 50 µL of the solution was mixed with 10 mM MOPS (pH 7.4, 100 µL) and LC-MS grade water (840 µL), to take background absorbance. LP3 or LP4 (10 µL, 100 µM) was then added to the solution (final volume of 1 mL). 200 µL of the final solution was scanned in the 280-600 nm region (0.01 cm cuvette, automatic background subtraction) with recording absorbance at 412 nm. Absorbance for each sample was calculated and the results were averaged and divided by 14,150/M·cm (extinction co-efficient of 2-nitro-5-thiobenzoate) and 2 (number of thiols in each peptide) to obtain final concentrations.

Bacterial colonisation

Peptides (200 µL, 100 µM) were incubated overnight in 10 mM MOPS, pH 7.4, 20°C. 50-µL aliquots of obtained solutions were mounted onto 8-well Nunc LabTek chambered glass slides, with buffer excess removed by blotting. Bacterial inocula were prepared in Mueller Hinton broth at A_{600} of 0.6, then diluted to 1:100 in the pre-warmed medium and 50 µL of this dilution was added to each well of the coated Nunc LabTek slides. Bacterial films formed after incubations over 16 hours were analysed using a Live/Dead BacLight bacterial viability stain kit (Molecular Probes, UK), and were visualized by a confocal laser scanning microscope (FV-1000, Olympus). Cell numbers, dead versus viable, were measured using ImageJ software.

Minimum inhibitory concentrations assay

Minimum inhibitory concentrations (MIC) were determined by broth microdilution on *P. aeruginosa* ATCC 27853, *E. coli* K12 and *S. aureus* ATCC 25723 according to the Clinical and Laboratory Standards Institute. Typically, 100 µl of 0.5 - 1 x 10^6 CFU per ml of each bacterium in Mueller Hinton broth was incubated in 96 well plates with 100 µL of serial two-fold dilutions of the peptides (final concentrations, 100-0 µM) at 37°C on a 3D orbital shaker. The absorbance was measured after peptide addition at 600 nm using a Victor 2 plate reader (Perkin Elmer). Minimum inhibitory concentrations (MICs) were defined as the lowest peptide concentration showing growth inhibition after 24 hours at 37°C. All tests were done in triplicate.

Haemolysis assay

To determine haemolytic activity each peptide was incubated with 10% (v/v) suspension of mammalilan (human, bovine) erythrocytes. The cells were rinsed 4 times in 10 mM PBS, pH 7.2, by repeated centrifugation and re-suspension (3 min, 3000 x g), and then were incubated at room temperature for 1 hour in either deionized water (fully haemolysed control), PBS or with peptide in PBS. After centrifugation (1 x 5 min, 10000 g), the supernatant was separated from the pellet and the absorbance was measured at 550 nm. The absorption of the suspension treated with deionized water defined complete haemolysis. All tests were done in triplicate.

Acknowledgements

We acknowledge funding from the UK's Department of Business, Innovation and Skills and from the European Community's Seventh Framework Programme, ERA-NET Plus, under Grant Agreement No. 217257.

Notes and references

[a]*National Physical Laboratory, Hampton Road, Teddington, TW11 0WL, UK. E-mail: max.ryadnov@npl.co.uk*
[b]*Current address: Université du Luxembourg, 7, Avenue des Hauts Fourneaux, L-4362 BELVAL, Luxembourg*
[‡]Contributed equally to this work.

1 S. Mitragotri and J. A. Lahann, *Nat. Mater*., 2009, **8**, 15.
2 L. L. Ling et al. *Nature*, **517**, 455.
3 C. D. Fjell, J. A. Hiss, R. E. W. Hancock and G. Schneider, *Nat Rev Drug Discov*., 2012, **11**, 37.
4 N. Faruqui, A. Bella, J. Ravi, S. Ray, B. Lamarre and M. G. Ryadnov, *J. Am. Chem. Soc.*, 2014, **136**, 7889.
5 T. Diu, N. Faruqui, T. Sjöström, B. Lamarre, H. F. Jenkinson, B. Su and M. G. Ryadnov, *Sci Rep*., 2014, **4**, 7122, DOI: 10.1038/srep07122.
6 A. L. Hook et al., *Nat. Biotechnol.*, 2012, **30**, 868.
7 M. C. Giano et al., *Nat Commun*., 2014, **5**, 4095.
8 J. Hasan, R. J. Crawford and E. P. Ivanova, *Trends Biotechnol*., 2013, **31**, 295.
9 H. Chu et al. *Science* 2012, **337**, 477.
10 N. Mookherjee and R. E. Hancock, *Cell Mol. Life Sci*., 2007, **64**, 922.
11 P. D. Rakowska et al. *Proc. Natl. Acad. Sci. USA*, 2013, **110**, 8918.
12 L. Ryan, et al. *J Biol. Chem*., 2013, **288**, 20162.
13 M. Zasloff, *Nature*, 2002, **415**, 389.

14 J. D. Hartgerink, E. Beniash and S. I. Stupp, *Science*, 2001, **294**, 1684.

15 S. Brahms, J. Brahms, G. Spach and A. Brack, *Proc. Natl. Acad. Sci. USA.* 1977, **74**, 3208.

16 M. G. Ryadnov and D. N. Woolfson, *J Am Chem. Soc*., 2007, **129**, 14074.

17 J. D. Morrisett, R. L. Jackson and A. M. Gotto, *Biochim. Biophys. Acta*, 1977, **472**, 93.

18 M. R. Hicks, J. Kowalski and A. Roger, *Chem. Soc. Rev*., 2010, **39**, 3380.

19 E. Cerasoli, J. Ravi, C. Gregor, R. Hussain, G. Siligardi, G., Martyna, J. Crain and M. G. Ryadnov, *Phys. Chem. Chem. Phys*., 2012, **14**, 1277.

20 K. E. Marshall, M. R. Hicks, T. L. Williams, S. V. Hoffmann, A. Rodger, T. R. Dafforn and L. C. Serpell, *Biophys. J*., 2010, **98**, 330.

21 M. G. Ryadnov, A. Bella, S. Timson and D. N. Woolfson, *J. Am. Chem. Soc*., 2009, **131**, 13240.

22 M. G. Ryadnov and D. N. Woolfson, *Angew Chem Int Ed.*, 2003, **42**, 3021.

23 B. Lamarre, J. Ravi and M. G. Ryadnov, *Chem. Commun*., 2011, **47**, 9045.

24 P. Enkhbayar, K. Hikichi, M. Osaki, R. H. Kretsinger and N. Matsushima, *Proteins*, 2006, **64**, 691.

25 M. N. Liang, S. P. Smith, S. J. Metallo, I. S. Choi, M. Prentiss, G. M. Whitesides, *Proc. Natl. Acad. Sci. USA*, 2000, **97**, 13092.

26 T. R. Jahn, O. S. Makin, K. L. Morris, K. E. Marshall, P. Tian, P. Sikorski, P. and L. C. Serpell, *J Mol. Biol*., 2010, **395**, 717.

27 C. J. C. de Haas, E. M. M. van Leeuwen, T. van Bommel, J. Verhoef, K. P. M. van Kessel and J. A. G. van Strijp, *Infect. Immun*., 2000, **68**, 1753.

28 D. S. Capstick, A. Jonaa, C. Hanke, J. Ortega and M. A. Elliot, *Proc. Natl. Acad. Sci. USA*, 2011, **108**, 9821.

29 B. L. Kagan, H. Janng, R. Capone, F. Teran Arce, S. Ramachandran, R. Lal and R. Nussinon. *Mol Pharm.* 2012, **9**, 708.

30 A. Makovitzki, D. Avrahami and Y. Shai, *Proc. Natl. Acad. Sci. USA*, 2006, **103**, 15997.

31 B. J. H. Kuipers and H. Gruppen, *J. Agric. Food Chem*., 2007, **55**, 5445.